ACS Biomaterials SCIENCE & ENGINEERING

Letter

Enhancing localized pesticide action through the plant foliage by silver-cellulose hybrid patches

Alejandro Alonso-Diaz, jordi Floriach-Clark, Judit fuentes, Montserrat Capellades, nuria sanchez-coll, and Anna Laromaine

ACS Biomater. Sci. Eng., **Just Accepted Manuscript** • DOI: 10.1021/acsbiomaterials.8b01171 • Publication Date (Web): 11 Jan 2019

ACS Publications

is published by the American Chemical Society. 1155 Sixteenth Street N.W., Washington, DC 20036

Enhancing localized pesticide action through the plant foliage by silver-cellulose hybrid patches.

Alejandro Alonso-Díaz[1], Jordi Floriach-Clark[2], Judit Fuentes[2], Montserrat Capellades[1], Núria S. Coll[1*], Anna Laromaine[2*]

[1] *Centre for Research in Agricultural Genomics (CRAG), CSIC-IRTA-UAB-UB, Campus UAB, Bellaterra, Barcelona, 08193, Spain.*

[2] *Institute of Material Science of Barcelona (ICMAB), CSIC, Carrer dels Til.lers, Campus UAB, Bellaterra, Barcelona, 08193, Spain.*

[*]*Corresponding authors: alaromaine@icmab.es, nuria.sanchez-coll@cragenomica.es*

KEYWORDS bacterial cellulose, silver nanoparticles, preventing infection, Nicotiana benthamiana, pseudomonas.

ABSTRACT:

Efficacy and efficiency of pesticide application in the field through the foliage still faces many challenges. There exists a mismatch between the hydrophobic character of the leaf and the active molecule, low dispersion of the pesticides on the leaves' surface, runoff loss and rolling down of the active molecules to the field, decreasing their efficacy and increasing their accumulation to the soil. We produced bacterial cellulose-silver nanoparticles hybrid patches by *in situ* thermal reduction under microwave irradiation in a scalable manner and obtaining AgNPs strongly anchored to the BC. Those hybrids increase the interaction of the pesticide (AgNPs) with the foliage and avoids runoff loss and rolling down of the nanoparticles. The positive anti-bacterial and anti-fungal properties were assessed *in vitro* against the bacteria *Escherichia coli* and two agro-economically relevant pathogens: the bacterium *Pseudomonas syringa*e and the fungus *Botrytis cinerea*. We showed *in vivo* inhibition of the infection in *Nicotiana benthamiana* and tomato leaves, as proven by the suppression of the expression of defense molecular markers and reactive oxygen species production. The hydrogel-like character of the bacterial cellulose matrix increases the adherence to the foliage of the patches.

Food security and the need to increase sustainably crop yields for a rapidly growing world population are among the greatest social and economic challenges of our century. The most extended agricultural practice to enhance crop yield is to increase host plant density, which in turn tends to increase the severity of plant diseases.[1] Most plant diseases occurring in agriculture are caused by fungal pathogens[2]. Diseases caused by pathogenic bacteria are less prevalent; but their effects are also devastating.[3]

To fight against pathogens, pesticides are effectively used in agriculture, securing a stable crop yield.[4] However, the efficacy and efficiency of the pesticides application in the field still faces many challenges. Pesticides sprayed through the leaves experience a mismatch of their hydrophobic character between the foliar tissue and the active molecule, which promotes low dispersion of the pesticides on the leaves' surface, a runoff loss and rolling down of the pesticides to the field, decreasing their efficacy and increasing their accumulation in the soil.

Several active ingredients with anti-pathogenic and anti-bacterial properties, such as several metal ions, have been explored in crops.[5] Currently, novel smart-based nanomaterials for pesticides have been developed since they can improve the low solubility issues of the active ingredients in water and its dispersions. The small size, big surface area and target modified properties of nanomaterials holds promise as nano-based pesticides.[6] Silver compounds have been commonly used as active ingredients in commercial pesticides[7], despite their toxic properties including DNA damage, inhibition of key enzyme activities or disruption of the bacterial membrane.[5,8,9] Silver compounds prepared as nanoparticles showed an increased efficacy and specificity as anti-bacterial and antimicrobial agents.[5,10] Price of those smart pesticides are not comparable to common bulk products currently used; however they suit high value applications such as vineyards, fruit trees or rare/valuable tree specimens.

We present a hybrid anti-bacterial and anti-fungal patch, which exploits the potential of smart-based nanomaterials; silver nanoparticles (AgNPs) as anti-bacterial active component. AgNPs are anchored to the bacterial cellulose matrix by *in situ* thermal reduction under microwave irradiation which prevents the release of the NPs to the environment and their runoff loss during application; improving the efficiency and environmental sustainability of this patch.

Cellulose is the most abundant biopolymer[11] and is the main constituent of the cell wall of plants.[12] However, cellulose can also be produced by different microorganisms, including bacterial species such as *Komagataeibacter xylinus (Kx). Kx* produces cellulose film as a sub-product of its metabolism, which has a hydrogel texture holding up to 90 times its weight on water.[13,14] Bacterial cellulose (BC) is obtained as an ultra-fine and highly pure tridimensional network exhibiting high water holding capacity, gel-like formulation[13] and biocompatibility, thus displaying high potential in regeneration and wound healing applications, Figure S1.[15] The bacterial cellulose matrix has similar chemical composition to the plant cellulose present in leaves but shows higher purity, crystallinity and water absorbance.[16,13] We took advantage of the hydrogel-like nature of the bacterial cellulose matrix to *in situ* synthesize and embedded AgNPs in order to confer anti-pathogenic properties to the patches. Different authors exploited the combination

of cellulose with silver nanoparticles, from impregnation[17,18] to *in situ* synthesis in cellulose, oxidized cellulose or combination with other materials[19–24] and evaluated them as anti-bacterial materials. However, the release of the NPs was commonly observed on those materials or not evaluated, even though its environmental hurdles. To avoid any runoff loss to the environment, we exploited the synthesis by *in situ* thermal reduction under microwave irradiation[25,26,27], in order to strongly anchor the AgNPs to the bacterial cellulose matrix.

Briefly, BC films were immersed in an $AgNO_3$ and PVP solution to ensure a homogeneous distribution of the precursor inside the cellulose network. After 10 min of microwave radiation, we observed the change of color of the BC films from translucent white to dark brown indicating the incorporation of the AgNPs into the cellulose scaffold (Figure 1a). SEM of BC-AgNPs hybrid films confirmed the homogeneous distribution of AgNPs within the film (Figure 1b) and by TEM we measured the diameter width of spherical shape metallic silver nanoparticles to 13±4 nm (Figure 1c). We analyzed the leaching process of BC-AgNPs hybrid films, immersing them in water for 14 days in gentle stirring (<60 rpm). We did not detect any change in the size, shape or color of the films. We semi-quantitatively measured BC-AgNPs leaching by analyzing the color change of the hybrid film by ImageJ software (grey scale) and we could not appreciate any change of color indicative of detachment of the particles from the hybrid films (Figure 1e). The content of silver on those films upon immersion was quantitatively measured by Coupled Plasma – Mass Spectroscopy (ICP-MS) and we did not observe any change. ICP-MS data confirmed that the release to the solution was of approximately 57 ppb in 14 days. Together, these data confirms the strong attachment of AgNPs to the BC matrix similar to what has been previously reported with iron oxide nanoparticles.[26] In addition, the release and degradation of the nanoparticles from the BC matrix is slow. The combination of the anti-pathogenic properties of the BC-AgNPs films and the slow release contributes to obtain a material that could be safer for the environment and more sustainable than most common pesticides used nowadays.

In order to obtain commercial products, it is important to have good reproducibility and scalability of the materials produced. We confirmed the reproducibility of 30 films produced in 5 different batches and synthesized by different users using different techniques such as thermogravimetric analysis, TEM, SEM and color analysis.

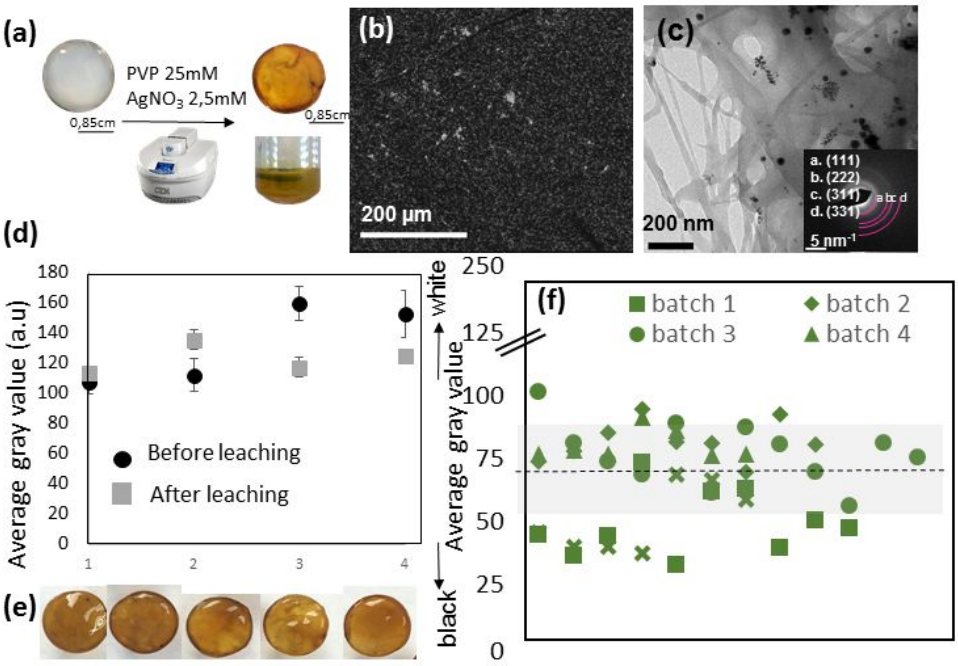

Figure 1. (a) Production of the AgNP-BC hybrid film by reduction of $AgNO_3$ assisted by microwave radiation; (b) SEM BSE image of AgNP-BC surface indicating high homogeneity; (c) TEM image and SEAD of AgNP-BC composite; (d) Qualitative measurement of the amount of Ag-NPs of the hybrids upon leaching. (e) Images of BC-AgNPs hybrids produced in the same batch. (f) Qualitative measurement of the reproducibility and amount of Ag-NPs in the BC-AgNPs hybrids from five batches. Average gray value is 69 (dashed line); ±1σ range is shaded; σ=19; n=30.

We analyzed the *in vitro* growth inhibitory effects of BC-AgNPs against a range of bacteria and fungi. We choose *Escherichia coli* as a reference species because of its known sensitivity against a wide range of antibiotics and *Pseudomonas syringae pv tomato* DC3000, causing the bacterial speck disease in tomato and a model plant pathogen. Growth inhibition of *E. coli* could be observed as a halo around a particular treatment (Figure 2a) and was quantified by measuring its diameter (1,2mm). In contrast, wet BC (BC-wet) film without AgNPs did not show any obvious inhibitory effect on bacterial growth. SEM observed higher bacterial densities in the positive control and BC-wet in comparison to the BC-AgNP treatment as shown in Figure 2b. As expected, gentamicin and $AgNO_3$ caused a transparent halo on the culture media. Figure 2c also shows that the BC-AgNPs film resulted in a transparent halo in *P. syringae* DC3000, demonstrating that this composite is also toxic for phytopathogenic bacteria. Even though BC-AgNPs films showed a low leaching and slow release of silver, we observed those films have anti-bacterial properties.

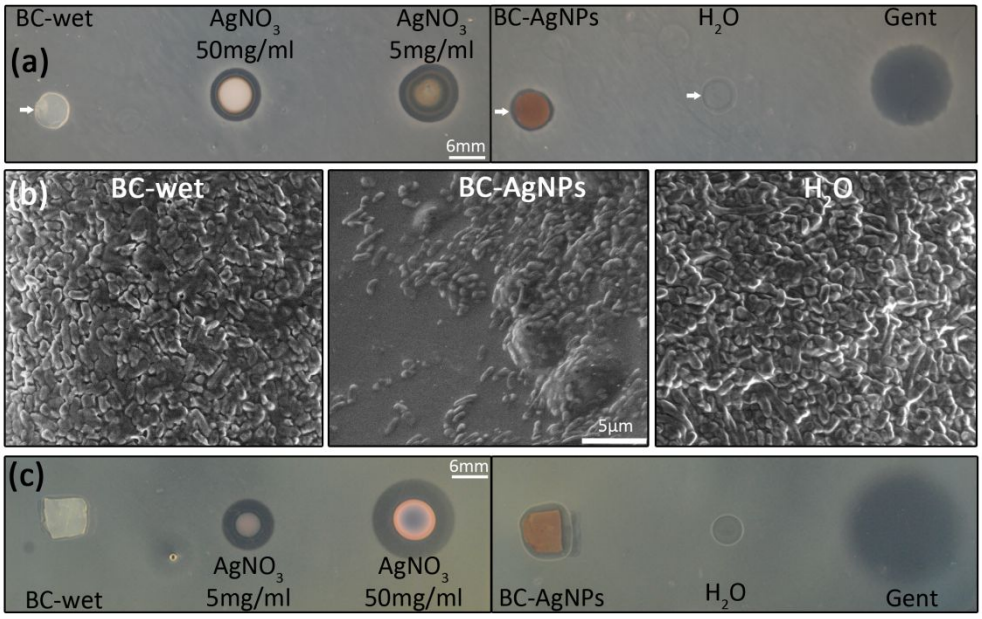

Figure 2: Toxicity assay of BC-AgNPs in bacteria (*E. coli* and *P. syringae*). (a) Toxicity assay using *E. coli*. strain OP50. Bacteria was growth in LB plate at 37ºC, and different treatments were applied: BC-wet (piece of 6 mm diameter), 5 µl $AgNO_3$ (50 mg/ml), 5 µl $AgNO_3$ (5 mg/ml), BC-AgNPs (piece of 6 mm diameter), 5 µl sterile miliQ water and 5 µl Gentamicin (10 mg/ml). (b) SEM images of BC-wet, BC-AgNPs and sterile miliQ water-treated bacteria were taken from areas pointed by white arrows. (c) Toxicity assay using *P. syringae* (DC3000). Bacteria were growth in KB plate at 28ºC, and different treatments were applied: BC-wet (piece of 6 mm diameter), 5 µl $AgNO_3$ (50 mg/ml), 5 µl $AgNO_3$ (5 mg/ml), BC-AgNPs (piece of 6 mm diameter), 5 µl sterile miliQ water and 5 µl Gentamicin (10 mg/ml). All photos were taken at 24 hours after treatment. Scale bar: 5 µm and 6 mm.

Potentially toxic effects of hybrid BC with silver nanoparticles are commonly tested only in bacteria and not assessed using fungal phytopathogens.[18,28–33] Previous reports showed that bacterial cellulose-copper oxide nanocomposites had anti-microbial activity against bacteria and yeast.[34] Therefore, to determine whether hybrid films were only toxic for bacteria or their effect could be extended to unrelated phytopathogens, we tested the patches against the plant pathogenic fungus *Botrytis cinerea* (B05.10 strain), the causal agent of gray mold disease and one of the most important fruit postharvest pathogens[35]. The fungal mycelium was allowed to develop for 9 days (Figure 3a) and after that, spores were extracted and quantified separately from a fixed area surrounding each treatment (Figure 3b). As expected, the strongest effect was caused by the AgNPs alone due to their ability to diffuse in the medium, which inhibited fungal colonization and spore production, as it has been reported in previous publications[36,37]. The BC-AgNPs also inhibited spore production ($4.75 \cdot 10^5$ spores/ml) compared to the control treatment ($3.6 \cdot 10^6$ spores/ml), and resulted in reduced fungal colonization, similar to what has been previously reported.[38] BC-wet alone did not significantly inhibit spore formation, although fungal colonization was slightly reduced. The growth

inhibition and toxicity of BC-AgNPs on the fungal mycelium can be clearly observed in the images shown in Figure 3c. The 5 mm² area adjacent to each different treatment (BC-AgNPs, BC-wet and untreated) was visualized using SEM. Untreated and BC-wet-treated mycelia showed no growth defects. In contrast, mycelia treated with BC-AgNPs had obvious signs of damage and cell death, with an apparent loss of turgor, deformation of the chitin cell walls and no spore production, indicating the toxicity reaction caused by the patch.

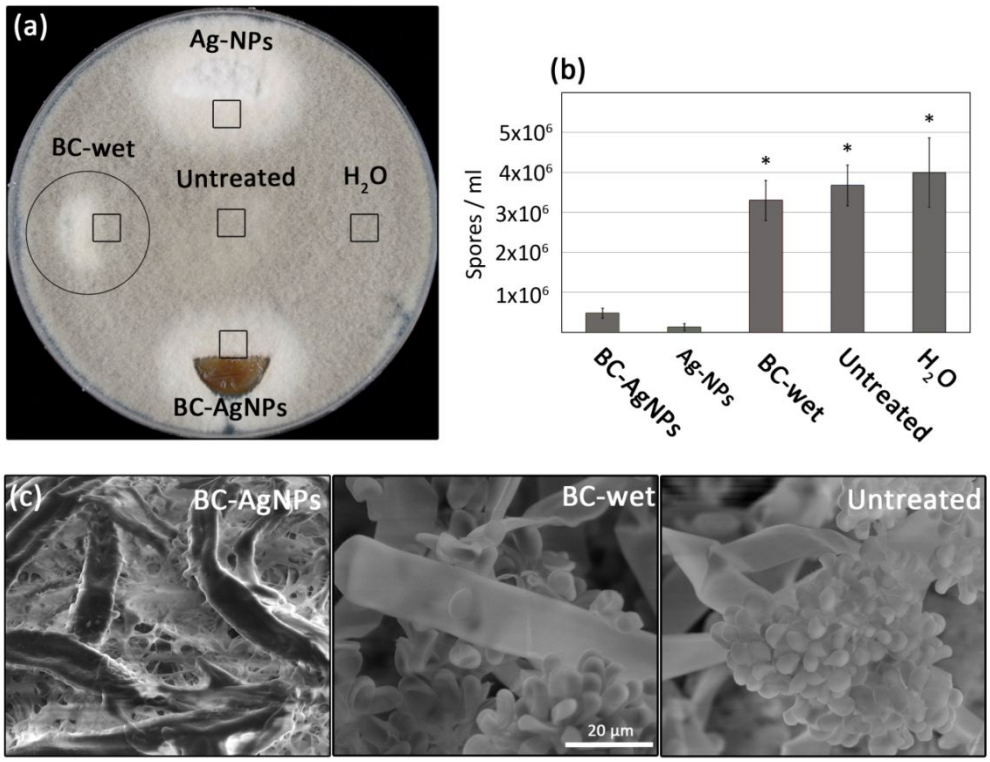

Figure 3: Toxicity assay of BC-AgNPs in *B. cinerea*. (a) Toxicity assay in PDA medium. 7,5 µl *B. cinerea* concentration 10^5 sp/ml inoculum were add in the center of the PDA plate: Top image corresponds to 15 µl AgNPs (0.53mg/ml), right image corresponds to BC-wet, left image corresponds to 15 µl sterile miliQ water and below image corresponds to BC-AgNPs. (b) Spore count using a toxicity assay plate. A piece of PDA plate of 2.7 cm diameter (marked with a circle) was excised for each treatment; BC-AgNPs, BC, AgNPs, untreated and sterile miliQ water. (c) SEM images were taken 9 days post infection (dpi) of a portion of the mycelia close to each treatment (marked with a square); BC-AgNPs, BC and untreated.

Then we evaluated the *in* vivo effects of BC-AgNPs; by infecting leaves of the model plant *Nicothiana benthamiana* with the bacterial pathogen *P. syringae* DC3000 on well-delimited 1-cm diameter areas. Then, the infected areas were left uncovered or covered for 6 days with BC film alone, or with BC-AgNPs film. *P. syringae* DC3000 caused a necrotic reaction on *N. benthamiana* in the uncovered control (Figure 4b and 4c). This reaction was mostly inhibited in the leaf area covered with BC-AgNPs, indicating that the film had a strong anti-bacterial effect on leaves. Interestingly, the BC film alone caused a slight inhibition of necrosis caused by

bacterial infection. This effect might be the result of additive factors including an altered environment for the bacteria (lower oxygen availability and reduced light intensity) and the material properties (porosity, thickness and roughness) added to the possibility that *Kx*-secreted molecules may have remained embedded in the BC matrix, providing supplementary anti-bacterial properties.
The reduction of necrosis correlated with a decrease of bacterial growth in the areas covered with BC-AgNPs and BC alone (Figure 4d). As expected, this inhibition of bacterial growth was more dramatic in BC-AgNPs than in BC-covered samples, in which only a minor, although significant, decrease of bacterial growth was observed. The anti-bacterial effect of BC-AgNPs was not restricted to N. *benthamiana* plants. We performed a *P. syringae* infection experiment using tomato, a crop of high agricultural value, observing similar effects (Figure S3). Curiously, in tomato we did not observe a significant decrease of bacterial growth in BC-treated samples.

Importantly, BC and BC-AgNP films strongly adhered when placed wet on the surface of leaves. These films stayed attached for long periods (more than 7 days) on the leaf surface under normal growth conditions (Figure 4a). In contrast, an analogous patch made of wet plant cellulose (filter paper) only stayed 1 day adhered to the leaves. As previously described, BC has high water absorbance and its composites retain this property. Therefore, we believe that the hydrogel consistency of the BC-AgNP film allows it to dry slowly; while it dries, it embeds the leaf trichomes (hair-like cells on the leaf adaxial surface) within the BC matrix, favoring the adhesion of the patches to the leaves. This strong adherence of BC may significantly contribute to the anti-pathogenic effects of the BC-AgNPs hybrid film, as it provides a stable, strongly anchored matrix in which the AgNPs can exert their toxic effect on the bacteria in close contact to the leaf, without detaching with time.

Anti-fungal activity of the BC-AgNPs and BC-wet alone in plants were tested on *N. benthamiana* leaves inoculated with a droplet of *B. cinerea* spore solution. Twenty-four hours after, the infection sites were covered with BC-AgNPs, BC-wet alone or left uncovered. After 6 days of treatment, effects were evaluated by taking pictures of the infected leaves (Figure 4e) and lesion size was measured (Figure 4f). The typical symptom caused by *B. cinerea* on *N. benthamiana* leaves is tissue necrosis, as it could be clearly observed in the uncovered control. Strikingly, the BC-AgNPs film totally inhibited the development of any visual fungal infection symptoms. In contrast, both BC-wet and uncovered treatment did not block disease progression. This indicates that the BC-AgNPs hybrid film has also a strong anti-fungal effect on plants.

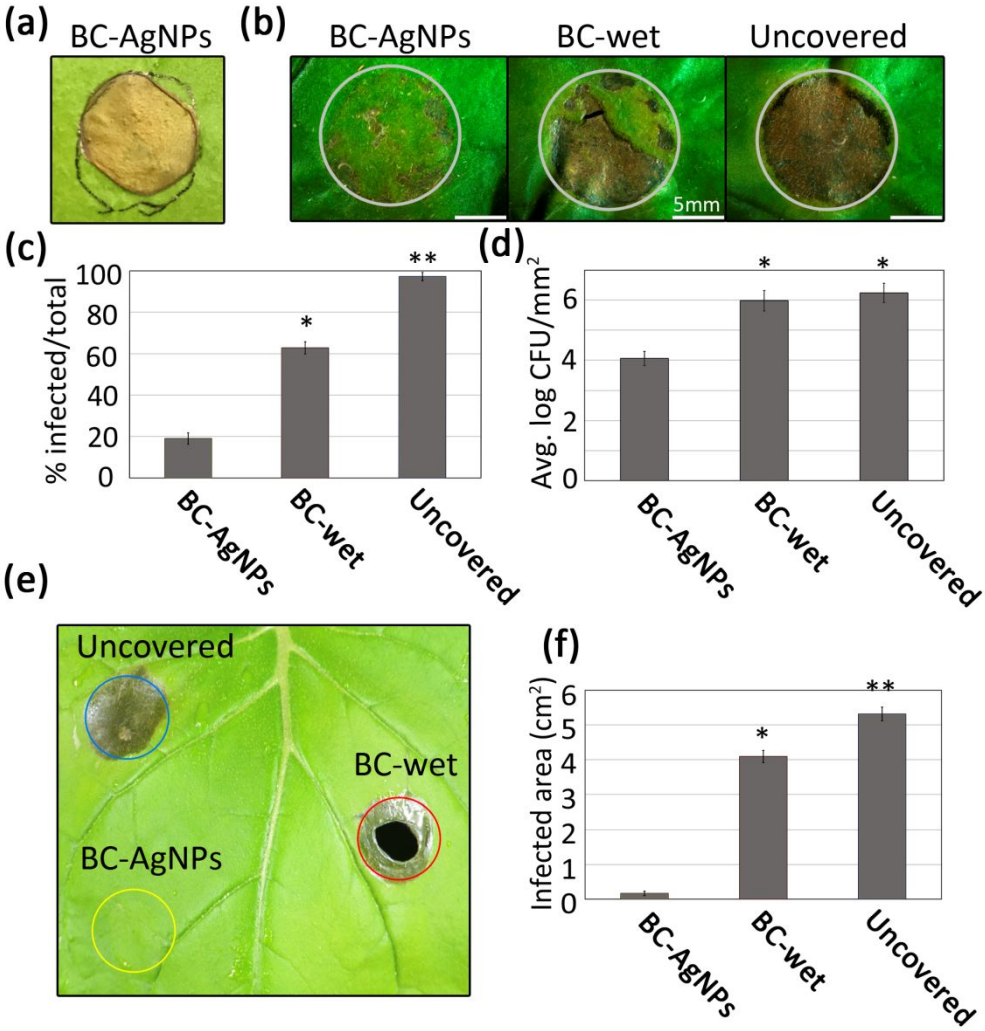

Figure 4: Anti-bacterial and anti-fungal activity of BC-AgNPs in *N. benthamiana* against *P. syringae* and *B. cinerea* (a) BC-AgNPs adhered to a *N. benthamiana* leaf (b) Three week-old *N. benthamiana* plants were infiltrated with *P. syringae* (DC3000) at an $O.D._{600}$ of 0.0008. After infiltration infected areas were covered with different treatments: BC-AgNPs, BC or left uncovered. Photos were taken 6dpi. (c) The area of necrotic tissue was measured with the ImageJ software at 6dpi d) Bacterial growth within a 1 cm-diameter infected area was measured as the average of colony forming units (CFUs) (logarithmic scale) per square millimeter of infected tissue. (e) Three week-old *N. benthamiana* leaves were infected with a 5 µl drop of 10^5 *B. cinerea* spores/ml and kept under 100 % humidity. After 24 h infected areas were covered with BC-AgNPs, BC-wet or left uncovered. After 6dpi the treatments were removed and digital pictures were taken. f) The area corresponding to the necrotic tissue was measured with ImageJ software at 6dpi.

The anti-pathogenic effect of BC-AgNPs could occur as a result of pathogen growth inhibition or by an enhancement of the plant defenses. To test a potential immune boosting effect of BC-AgNPs on bacterial infection, we quantified the expression of *PATHOGENESIS-RELATED 1a* (*PR1a*), a plant defense marker gene [39] *PR1a* was expressed in BC-AgNPs -treated infected tissue, although to very low levels, 18 times lower than the uncovered control (Figure 5a). The BC-AgNPs patch strongly inhibited pathogenic bacteria perception and the subsequent immune response of the plant. BC-wet film alone also caused partial inhibition of *PR1a* expression to approximately 1.6 times lower than untreated leaf levels. This result correlates with the decreased extent of pathogen-triggered necrosis observed upon infection in BC-AgNPs-covered leaf areas when compared to the untreated control (Figure 5a and 5e).

In parallel, we analyzed gene expression profiles of *HOMEOBOX 1* (*HB1*) and *HARPIN-INDUCED GENE* (*HIN1*) after fungal infection with *B. cinerea*. *HBI* is a gene which is expressed in pathogen-induced cell death and its expression is dependent on jasmonic acid signaling, which is activated upon necrotrophic fungal infection[40]. On the other hand, *HIN1* is a marker of pathogen-triggered cell death[41]. Figure 5b shows that these genes are upregulated in inoculated tissue that was either uncovered or covered with tape, indicating pathogen perception and response by the plant. In contrast, BC-AgNPs-covered tissue shows minor upregulation of the two marker genes, suggesting that BC-AgNPs may directly inhibit *B. cinerea* infection, previous to the activation of the plant immune system. This indicates that fungal growth arrest may occur at very early stages of infection.

Recognition of a pathogen by a plant results in a rapid burst of reactive oxygen species (ROS), which can be measured as an output of plant defense responses.[42] Previous reports showed also an increase of ROS upon exposure of AgNPs to some plants.[43] Production of hydrogen peroxide (H_2O_2), one of the main ROS produced by the plant upon pathogen infection, was visualized in leaf areas infected with *P. syringae* DC3000 using 3, 3 –diaminobenzidine (DAB) staining. Figure 5c-d clearly shows that infection results in accumulation of H_2O_2 in uncovered tissue, when compared to uninfected or mock-inoculated leaf tissue ($MgCl_2$). In contrast, *P. syringae*-inoculated tissue covered with BC-AgNPs displays a drastic reduction on H_2O_2 accumulation. This observation corroborates the previous findings indicating that defense responses are not induced in inoculated tissue covered with BC-AgNPs. Together, these data corroborate that the anti-bacterial effect of BC-AgNPs does not result from enhanced plant defense responses. BC-wet film alone did not prevent ROS accumulation in the inoculated tissue, which is not surprising, considering that the extent of bacterial growth inhibition caused by this film is minor when compared to BC-AgNPs. Previous reports indicated an increase of ROS caused by nanoparticle exposure,[43] potentially harmful for living cells and tissues. The fact that the leaf treatment with the BC-AgNPs hybrid does not result in ROS production might constitute another indication that AgNPs are not released from the BC matrix, avoiding any effects derived from AgNPs treatment alone and preventing their release to the environment".

ROS produced as a result of *B. cinerea* infection were absent in the BC-AgNPs-covered sample; in contrast to inoculated samples covered with BC-wet which showed ROS production levels comparable to those of the uncovered control (Figure 5e and 5f).These data corroborate our previous observation indicating that BC-AgNPs completely blocks fungal invasion at very early stages. Thanks to this rapid elimination of the pathogen, the plant does not even perceive it and thus, unnecessary defense reactions are prevented.

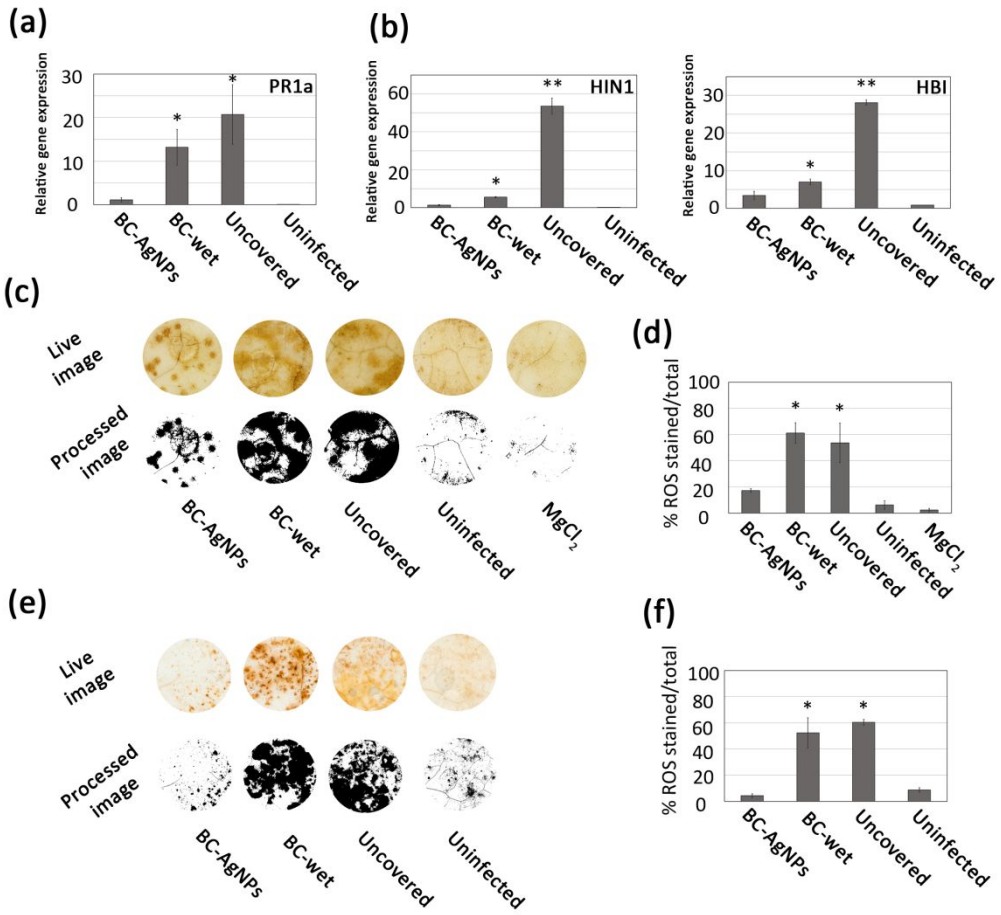

Figure 5: Defense molecular markers and reactive oxygen species (ROS) (a-b) Quantitative PCR (qPCR) analysis of defense marker genes. Three week-old N. benthamiana plants were infiltrated with (a)P. syringae DC3000 at an O.D.600 of 0.001, (b)Three week-old plants were sprayed with either 105 spores/ml of B. cinerea and keep for 24 hours under 100% humidity.Then, the infected zones were covered with the different treatment (BC-AgNPs, BC-wet and uncovered) during 12 hours and then RNA was extracted. qPCR was performed with specific primers for N. benthamiana (a) PR1a, (b) HIN1, HBI and Tubulin (control) genes as described in Material and Methods. (c) to (f) ROS production analysis. (c) Three week-old *N. benthamiana* leaves were infected with *P. syringae* DC3000 (*avrRpm1*) at an $O.D._{600}$ of 0.01 and then covered with: BC-AgNPs and BC or left uncovered. As a negative control uninfected tissue was used. After 12 hpi the infected zones with different treatments were stained using the H_2O_2 stain 3,3′-diaminobenzidine (DAB). Stained leaves were imaged using a digital camera. (d) Quantification of

the images shown in (c) as the percentage of DAB stain present using the Image J software. (e) Three week-old *N. benthamiana* leaves were infected with *B. cinerea* at 10^5 spores/ml concentration and keep for 24 hours under 100% humidity. Then, the infected zones were covered with BC-AgNPs, BC-wet and uncovered and after 12 hpi. The infected zones and uninfected control were stained using DAB and images were taken using a digital camera. Previously staining leaves were processed with ImageJ. (f) Quantification of the images shown in (e) as the percentage of DAB stain present using the ImageJ software.

In summary, we have developed environmentally friendly nanocomposite patches based on bacterial cellulose and silver nanoparticles in a reproducible and scalable manner; with positive results against the bacteria *Escherichia coli* and *Pseudomonas syringae* and the fungus *Botritis cinerea.* Thanks to their hydrogel-like consistency, we obtained a strong adherence to *N. benthamiana* leaves inoculated *B. cinerea* spore solution. We confirmed the pathogen inhibitory properties of the material by quantitative gene expression profiling of various plant defense marker genes, and by reactive oxygen species quantification in the inoculated tissue, showing no defense response activation probably due to an early neutralization of the pathogen on site by the nanocomposite. The slow release of silver nanoparticles from the bacterial cellulose makes this material potentially safer for the environment than most current pesticides. Thus, this bacterial cellulose silver nanoparticle composite shows promise as a new generation pesticide, potentially overcoming bottlenecks to increase efficacy and efficiency of current foliar pesticides.

Supporting Information

Materials and Methods for the production of BC and BC hybrids and their characterization. Experimental protocols for the evaluation of the BC hybrids on pathogens and plants.

Conflicts of interest

There are no conflicts of interest to declare.

Acknowledgements

We acknowledge financial support from the Spanish Ministry of Economy and Competitiveness (MINECO) with grants 2016-78002-R (AGL) and RyC 2014-16158 (NSC), MAT2015-64442-R, FIP and through the "Severo Ochoa Programme for Centres of Excellence in R&D" (SEV-2015-0533 and SEV-2015-0496). This work was also supported by the CERCA Programme / Generalitat de Catalunya, the Generalitat de Catalunya for the 2017SGR765 project. The authors would like to thank all members of the "bacterial plant diseases and cell death" lab for helpful comments.

References

(1) Sundström, J. F.; Albihn, A.; Boqvist, S.; Ljungvall, K.; Marstorp, H.; Martiin, C.; Nyberg, K.; Vågsholm, I.; Yuen, J.; Magnusson, U. Future Threats to Agricultural Food Production Posed by Environmental Degradation, Climate Change, and Animal and Plant Diseases - a Risk Analysis in Three Economic and Climate Settings. *Food Secur.* **2014**, *6* (2), 201–215. https://doi.org/10.1007/s12571-014-0331-y.

(2) Agrios, G. N. *Plant Pathology. Quinta Edición. Academic Press. Nueva York.*; 2005. IBSN: 0120445654

(3) V. Rajesh Kannan, K. K. B. *Sustainable Approaches to Controlling Plant Pathogenic Bacteria*; 2015. IBSN: 9781482240542

(4) FAO. *Food and Agriculture Organization, the International Code of Conduct on Pesticide Management*; 2014. IBSN: 9789251085486

(5) Lemire, J. a; Harrison, J. J.; Turner, R. J. Antimicrobial Activity of Metals: Mechanisms, Molecular Targets and Applications. *Nat. Rev. Microbiol.* **2013**, *11* (6), 371–384. https://doi.org/10.1038/nrmicro3028.

(6) Zhao, X.; Cui, H.; Wang, Y.; Sun, C.; Cui, B.; Zeng, Z. Development Strategies and Prospects of Nano-Based Smart Pesticide Formulation. *J. Agric. Food Chem.* **2017**. https://doi.org/10.1021/acs.jafc.7b02004.

(7) Agency, U. S. E. P. Silver in Business. 1992.

(8) Oka, H.; Tomioka, T.; Tomita, K.; Nishino, a; Ueda, S. Inactivation of Enveloped Viruses by a Silver-Thiosulfate Complex. *Met. Based. Drugs* **1994**, *1* (5–6), 511. https://doi.org/10.1155/MBD.1994.511.

(9) Jo, Y.-K.; Kim, B. H.; Jung, G. Antifungal Activity of Silver Ions and Nanoparticles on Phytopathogenic Fungi. *Plant Dis.* **2009**, *93* (10), 1037–1043. https://doi.org/10.1094/PDIS-93-10-1037.

(10) Hajipour, M. J.; Fromm, K. M.; Akbar Ashkarran, A.; Jimenez de Aberasturi, D.; Larramendi, I. R. de; Rojo, T.; Serpooshan, V.; Parak, W. J.; Mahmoudi, M. Antibacterial Properties of Nanoparticles. *Trends Biotechnol.* **2012**, *30* (10), 499–511. https://doi.org/10.1016/j.tibtech.2012.06.004.

(11) Jonas, R.; Farah, L. F. Production and Application of Microbial Cellulose. *Polym. Degrad. Stab.* **1998**, *59* (1–3), 101–106. https://doi.org/10.1016/S0141-3910(97)00197-3.

(12) Heredia, A.; Jiménez, A.; Guillén, R.; Guillénn, R. Composition of Plant Cell Walls. *Z. Lebensm. Unters. Forsch.* **1995**, *200* (1), 24–31. https://doi.org/10.1007/BF01192903.

(13) Zeng, M.; Laromaine, A.; Roig, A. Bacterial Cellulose Films: Influence of Bacterial Strain and Drying Route on Film Properties. *Cellulose* **2014**, *21* (6), 4455–4469. https://doi.org/10.1007/s10570-014-0408-y.

(14) Hestrin, S.; Schramm, M. Synthesis of Cellulose by Acetobacter Xylinum. 2. Preparation of Freeze-Dried Cells Capable of Polymerizing Glucose to Cellulose*. *Biochem. J.* **1954**, *58* (2), 345–352. https://doi.org/10.1042/bj0580345.

(15) Boateng, J.; Catanzano, O. Advanced Therapeutic Dressings for Effective Wound Healing - A Review. *J. Pharm. Sci.* **2015**, *104* (11), 3653–3680.

https://doi.org/10.1002/jps.24610.
(16) Klemm, D.; Kramer, F.; Moritz, S.; Lindström, T.; Ankerfors, M.; Gray, D.; Dorris, A. Nanocelluloses: A New Family of Nature-Based Materials. *Angew. Chemie - Int. Ed.* **2011**, *50* (24), 5438–5466. https://doi.org/10.1002/anie.201001273.
(17) Mohite, B. V.; Patil, S. V. In Situ Development of Nanosilver-Impregnated Bacterial Cellulose for Sustainable Released Antimicrobial Wound Dressing. *Journal of Applied Biomaterials & Functional Materials*. 2016, pp e53-8. https://doi.org/10.5301/jabfm.5000257.
(18) Maneerung, T.; Tokura, S.; Rujiravanit, R. Impregnation of Silver Nanoparticles into Bacterial Cellulose for Antimicrobial Wound Dressing. *Carbohydr. Polym.* **2008**, *72* (1), 43–51. https://doi.org/10.1016/j.carbpol.2007.07.025.
(19) Wu, C. N.; Fuh, S. C.; Lin, S. P.; Lin, Y. Y.; Chen, H. Y.; Liu, J. M.; Cheng, K. C. TEMPO-Oxidized Bacterial Cellulose Pellicle with Silver Nanoparticles for Wound Dressing. *Biomacromolecules* **2018**, *19* (2), 544–554. https://doi.org/10.1021/acs.biomac.7b01660.
(20) Yang, G.; Yao, Y.; Wang, C. Green Synthesis of Silver Nanoparticles Impregnated Bacterial Cellulose-Alginate Composite Film with Improved Properties. *Mater. Lett.* **2017**, *209*, 11–14. https://doi.org/10.1016/j.matlet.2017.07.097.
(21) De Moura, M. R.; Mattoso, L. H. C.; Zucolotto, V. Development of Cellulose-Based Bactericidal Nanocomposites Containing Silver Nanoparticles and Their Use as Active Food Packaging. *J. Food Eng.* **2012**, *109* (3), 520–524. https://doi.org/10.1016/j.jfoodeng.2011.10.030.
(22) Li, Y. T.; Lin, S. Bin; Chen, L. C.; Chen, H. H. Antimicrobial Activity and Controlled Release of Nanosilvers in Bacterial Cellulose Composites Films Incorporated with Montmorillonites. *Cellulose* **2017**, *24* (11), 4871–4883. https://doi.org/10.1007/s10570-017-1487-3.
(23) Kishanji, M.; Mamatha, G.; Obi Reddy, K.; Varada Rajulu, A.; Madhukar, K. In Situ Generation of Silver Nanoparticles in Cellulose Matrix Using Azadirachta Indica Leaf Extract as a Reducing Agent. *Int. J. Polym. Anal. Charact.* **2017**, *22* (8), 734–740. https://doi.org/10.1080/1023666X.2017.1369612.
(24) Rieger, K. A.; Cho, H. J.; Yeung, H. F.; Fan, W.; Schiffman, J. D. Antimicrobial Activity of Silver Ions Released from Zeolites Immobilized on Cellulose Nanofiber Mats. *ACS Appl. Mater. Interfaces* **2016**, *8* (5), 3032–3040. https://doi.org/10.1021/acsami.5b10130.
(25) Gonzalez-Moragas, L.; Yu, S. M.; Murillo-Cremaes, N.; Laromaine, A.; Roig, A. Scale-up Synthesis of Iron Oxide Nanoparticles by Microwave-Assisted Thermal Decomposition. *Chem. Eng. J.* **2015**, *281*, 87–95. https://doi.org/10.1016/j.cej.2015.06.066.
(26) Zeng, M.; Laromaine, A.; Feng, W.; Levkin, P. A.; Roig, A. Origami Magnetic Cellulose: Controlled Magnetic Fraction and Patterning of Flexible Bacterial Cellulose. *J. Mater. Chem. C* **2014**, *2* (31), 6312–6318. https://doi.org/10.1039/C4TC00787E.
(27) Xu, Y.-J.; Wang, J.-Y.; Zuo, L.-G.; Qian, X. Rapid Microwave-Assisted

Synthesis and Characterization of Cellulose Fiber Containing Silver Nanoparticles in Alkaline Aqueous Solution. *Science of Advanced Materials*. 2016, pp 1585–1594. https://doi.org/10.1166/sam.2016.2771.

(28) Wu, J.; Zheng, Y.; Song, W.; Luan, J.; Wen, X.; Wu, Z.; Chen, X.; Wang, Q.; Guo, S. In Situ Synthesis of Silver-Nanoparticles/Bacterial Cellulose Composites for Slow-Released Antimicrobial Wound Dressing. *Carbohydr. Polym.* **2014**, *102* (1), 762–771. https://doi.org/10.1016/j.carbpol.2013.10.093.

(29) Yang, G.; Xie, J.; Hong, F.; Cao, Z.; Yang, X. Antimicrobial Activity of Silver Nanoparticle Impregnated Bacterial Cellulose Membrane: Effect of Fermentation Carbon Sources of Bacterial Cellulose. *Carbohydr. Polym.* **2012**, *87* (1), 839–845. https://doi.org/10.1016/j.carbpol.2011.08.079.

(30) Barud, H. S.; Regiani, T.; Marques, R. F. C.; Lustri, W. R.; Messaddeq, Y.; Ribeiro, S. J. L. Antimicrobial Bacterial Cellulose-Silver Nanoparticles Composite Membranes. *J. Nanomater.* **2011**, *2011*. https://doi.org/10.1155/2011/721631.

(31) Maria, L. C. S.; Santos, A. L. C.; Oliveira, P. C.; Valle, A. S. S.; Barud, H. S.; Messaddeq, Y.; Ribeiro, S. J. L. Preparation and Antibacterial Activity of Silver Nanoparticles Impregnated in Bacterial Cellulose. *Polímeros* **2010**, *20* (1), 72–77. https://doi.org/10.1590/S0104-14282010005000001.

(32) Li, Z.; Wang, L.; Chen, S.; Feng, C.; Chen, S.; Yin, N.; Yang, J.; Wang, H.; Xu, Y. Facilely Green Synthesis of Silver Nanoparticles into Bacterial Cellulose. *Cellulose* **2015**, *22* (1), 373–383. https://doi.org/10.1007/s10570-014-0487-9.

(33) Yang, J.; Liu, X.; Huang, L.; Sun, D. Antibacterial Properties of Novel Bacterial Cellulose Nanofiber Containing Silver Nanoparticles. *Chinese J. Chem. Eng.* **2013**, *21* (12), 1419–1424. https://doi.org/10.1016/S1004-9541(13)60636-9.

(34) Araújo, I. M. S.; Silva, R. R.; Pacheco, G.; Lustri, W. R.; Tercjak, A.; Gutierrez, J.; Júnior, J. R. S.; Azevedo, F. H. C.; Figuêredo, G. S.; Vega, M. L.; Ribeiro, S. J. L.; Barud, H. S. Hydrothermal Synthesis of Bacterial Cellulose–copper Oxide Nanocomposites and Evaluation of Their Antimicrobial Activity. *Carbohydr. Polym.* **2017**, *179* (2018), 341–349. https://doi.org/10.1016/j.carbpol.2017.09.081.

(35) Oirdi, M. El; Bouarab, K. Plant Signalling Components EDS1 and SGT1 Enhance Disease Caused by the Necrotrophic Pathogen Botrytis Cinerea. **2007**, *175* (1), 131–139. https://doi.org/10.1111/j.1469-8137.2007.02086.x.

(36) Villamizar-Gallardo, R.; Cruz, J. F. O.; Ortíz, O. O. Fungicidal Effect of Silver Nanoparticles on Toxigenic Fungi in Cocoa. *Pesqui. Agropecu. Bras.* **2016**, *51* (12), 1929–1936. https://doi.org/10.1590/S0100-204X2016001200003.

(37) Kim, S. W.; Jung, J. H.; Lamsal, K.; Kim, Y. S.; Min, J. S.; Lee, Y. S. Antifungal Effects of Silver Nanoparticles (AgNPs) against Various Plant Pathogenic Fungi. *Mycobiology* **2012**, *40* (1), 53–58. https://doi.org/10.5941/MYCO.2012.40.1.053.

(38) Adepu, S.; Khandelwal, M. Broad-Spectrum Antimicrobial Activity of Bacterial Cellulose Silver Nanocomposites with Sustained Release. *J. Mater. Sci.* **2018**, *53* (3), 1596–1609. https://doi.org/10.1007/s10853-017-1638-9.

(39) Ward, E. R.; Payne, G. B.; Moyer, M. B.; Williams, S. C.; Dincher, S. S.; Sharkey, K. C.; Beck, J. J.; Taylor, H. T.; Ahl-Goy, P.; Meins, F.; Ryals, J.

Differential Regulation of Beta-1,3-Glucanase Messenger RNAs in Response to Pathogen Infection. *Plant Physiol.* **1991**, *96* (2), 390–397. https://doi.org//91 /96/0390/08/$01 .00/0.

(40) Yoon, J.; Chung, W.; Choi, D. Jasmonic Acid-Dependent Positive Regulator of Pathogen-Induced Plant Cell Death. *New Phytol.* **2009**, *184* (1), 71–84. https://doi.org/10.1111/j.1469-8137.2009.02967.x.

(41) Pontier, D.; Tronchet, M. Activation of Hsr 203, a Plant Gene Expressed during Incompatible Plant-Pathogen Interactions, Is Correlated with Programmed Cell Death. *Mol Plant Microbe Interact* **1998**, *11* (6), 544–554. https://doi.org/10.1094/MPMI.1998.11.6.544.

(42) Torres, M. A. ROS in Biotic Interactions. *Physiol. Plant.* **2010**, *138* (4), 414–429. https://doi.org/10.1111/j.1399-3054.2009.01326.x.

(43) Pratley, J. E.; Haig, T. *Metal-Based Nanomaterials and Oxidative Stress in Plants: Current Aspects and Overview.*; 2018; Vol. 26. https://doi.org/10.1007/978-3-319-76708-6.

Enhancing localized pesticide action through the plant foliage by silver-cellulose hybrid patches.

Alejandro Alonso-Díaz[1], Jordi Floriach-Clark[2], Judit Fuentes[2], Montserrat Capellades[1], Núria S. Coll[1*], Anna Laromaine[2*]

[1] *Centre for Research in Agricultural Genomics (CRAG), CSIC-IRTA-UAB-UB, Campus UAB, Bellaterra, Barcelona, 08193, Spain.*

[2] *Institute of Material Science of Barcelona (ICMAB), CSIC, Campus UAB, Bellaterra, Barcelona, 08193, Spain.*

[*]*Corresponding authors: alaromaine@icmab.es, nuria.sanchez-coll@cragenomica.es*

TOC